



OPEN Promoting the remediation of contaminated soils using biochar in combination with bioaugmentation and phytoremediation techniques

Valentina Mazzurco-Miritana^{1,2}, Laura Passatore^{1✉}, Massimo Zacchini^{1,8}, Fabrizio Pietrini^{1,8}, Eleonora Peruzzi³, Serena Carloni¹, Ludovica Rolando⁴, Gian Luigi Garbini⁴, Anna Barra Caracciolo⁴, Vanesa Silvani⁵, Maria Cristina Moscatelli⁶, Rosita Marabottini⁶, Luisa Massaccesi⁷, Sara Marinari⁶ & Isabel Nogués¹

Pollutants in soils are detrimental to ecosystems and agricultural production and may also be a pressing threat to human health. In this context, biochar could be used as part of nature-based solutions to remediate polluted areas. In this work, a series of innovative biochar-based strategies were tested in a soil contaminated by hydrocarbons C_{>12} and copper (Cu) to investigate their effectiveness in soil decontamination and revegetation potential. Specifically, biochar was applied to soil alone (SB) or combined with bioaugmentation (SBB) and/or phytoremediation (SBP and SBBP) techniques. Overall results showed that after nine months (T9) biochar added to soil increased hydrocarbon degradation to 66.7% with respect to control soil (46%, natural attenuation). Moreover, the biochar in combination with a microbial consortium and/or plants significantly increased hydrocarbon removal by up to 90%. Concurrently, the fraction of Cu associated with organic matter, characterized by low bioavailability, increased significantly (1.4–2-fold) when biochar was applied. Soil microbial abundance increased over time in all conditions, reaching highest values in SBB and SBBP. This was associated with the higher levels of available phosphorus in the soil. The consortium's presence enhanced plant growth compared to SB. On the contrary, plants grown on contaminated soil alone were not able to survive until the end of the experiment. Overall, the results of this work make a significant contribution to the understanding of the interaction of biochar with contaminants, plants and microorganisms, providing a useful tool for future brownfield revegetation/remediation programs.

Keywords *Melilotus officinalis*, Soil bioremediation, Hydrocarbons, Copper, Bioavailability, Bioactivators

Soil contamination is a major global issue, and both heavy metals and organic pollutants can cause significant environmental problems. Pollutants in soils are detrimental to ecosystems and agricultural production and may also be a pressing threat to human health. Therefore, it is crucial to find nature-based solutions for remediating polluted areas. In this context, biochar, a vegetal black carbon produced by the pyrolysis of biomass, has received much attention due to its physicochemical characteristics, the possibility of valorizing this material as a by-product of biomass conversion and to its potential as a carbon sequestration material¹. Biochar has been proposed as soil amendment in agriculture, demonstrating its positive effects on soil fertility and water retention potential^{2–4}. Novel applications for water treatment and soil remediation are being explored,

¹Research Institute on Terrestrial Ecosystems, National Research Council (IRET-CNR), SP 35d, km 0.7, 00010 Montelibretti, Rome, Italy. ²Department of Energy Technology and Renewables, Italian National Agency for New Technologies, Energy and Sustainable Economic Development (ENEA), via Anguillarese 301, 00123 Rome, Italy. ³Research Institute on Terrestrial Ecosystems, National Research Council (IRET-CNR), via Moruzzi 1, 56124 Pisa, Italy. ⁴Water Research Institute, National Research Council (IRSA-CNR), SP 35d, km 0.7, 00010 Montelibretti, Rome, Italy. ⁵Instituto de Biodiversidad y Biología Experimental y Aplicada, CONICET-UBA, Facultad de Ciencias Exactas y Naturales, C1428EGA, Universidad de Buenos Aires, Buenos Aires, Argentina. ⁶Department for Innovation in Biological, Agrofood and Forest systems, University of Tuscia, Via San Camillo de Lellis, 01100 Viterbo, Italy. ⁷Institute for Agriculture and Forestry Systems in the Mediterranean, National Research Council (ISAFOM-CNR), Via della Madonna Alta, 128, 06128 Perugia, Italy. ⁸NBFC, National Biodiversity Future Center S.C.a.R.L., Piazza Marina 61 (C/O Palazzo Steri), 90133 Palermo, Italy. ✉email: laura.passatore@cnr.it

presented as interesting solutions in the context of a circular and carbon neutral economy^{5–8}. The high surface area pore structure and high adsorption capacity of biochar enable toxic compounds such as heavy metals to immobilize^{9,10}. In addition, from an ecological perspective, the growth and reproduction of microorganisms can be supported by the presence of biochar pores, which provide a habitat, and by the presence of available nutrients and energy to sustain their growth¹¹. Soil microbial communities play important ecological roles in terrestrial ecosystems such as organic matter decomposition, nutrient cycling, and organic pollutant degradation¹². They are influenced by the physicochemical characteristics of soil such as pH, moisture, organic carbon, and nutrient content, as well as by contaminant presence and soil amendments. Microbial decontamination of petroleum hydrocarbon (PHC) contaminated soils has been extensively studied¹³ and has been described as a cheap and effective strategy to recover contaminated soils¹⁴. Several microorganisms and consortia have been identified to degrade organic hydrocarbons in soils¹³ and they can be promisingly used in bioaugmentation applications¹⁵ for remediation of contaminated soils¹⁶.

In recent years, several studies and reviews have focused on the possibility of using the combined action of bioaugmentation and biochar as an effective strategy for microbial remediation of contaminated soils^{14,17–20}. Tu et al.²¹ observed that the application of biochar and *Pseudomonas* sp. decreased the lability and bioavailability of both Cd and Cu, especially at the highest application rates. In other studies, the immobilization of microorganisms on biochar has been shown to be advantageous for hydrocarbon remediation with higher removal values and promotion of microbial populations^{22,23}. Zhang et al.²³ demonstrated that, after 60 days of treatment, the concentration of C12–18 hydrocarbons in the soil decreased, highlighting a removal efficiency of 30–58%. Biochar has also been recommended as a carrier for microorganisms. In fact, biochar has been demonstrated to enhance the persistence, survival and colonization of microbial *inocula* in soil and plant roots^{24,25}. This aspect has mostly been studied for agronomic applications. More recently, it has garnered attention for its potential in soil remediation^{26–28}.

Furthermore, plants can be used to reduce, eliminate, and transform organic toxic compounds and to immobilize and/or accumulate heavy metals^{29,30}. Contaminant immobilization and degradation are particularly enhanced by plant root and soil microbial interactions³¹. Revegetating contaminated soils amended with organic matter and/or biochar can result in significant reductions in contaminant mobility in the soil³². However, a recent review highlighted that biochar used in synergy with the presence of plants could play a dual role in heavy metal contaminated soils, i.e. phytoextraction or phytostabilisation, depending on the type of biochar and the rate of application³³. Revegetation of contaminated soil presents other advantages: (i) improves soil water-holding capacity, (ii) reduces the volume of overland runoff and soil erosion, (iii) facilitates soil aeration, (iv) increases the content of available carbon through the decomposition of plant residue and the release of root exudates, and (v) can help to restore proper ecological functions by improving and stimulating the diversity and functionality of soil microorganisms³⁴.

Several studies about soil remediation have focused on the effect of a single strategy e.g. biochar soil amendment, bioremediation with microorganisms, phytoremediation or of a combination of two of them^{35–39}. However, the combined use of biochar–microorganism–plant and a direct comparison among these remediation techniques have received little attention so far. In this framework, Xiang et al.⁴⁰ have recently highlighted the necessity of exploring all facets of biochar–microorganism–plant associations in remediating organic contaminated soils and in particular those simultaneously polluted by organic and metal ones.

This work aims to study the effect of biochar amendment, alone and in combination with bioremediation techniques, on soil pollution (hydrocarbons and Cu) and on its revegetation potential. Reports from countries across Europe indicate that heavy metals and mineral oil are the most frequent soil contaminants at investigated sites. Among them, polycyclic aromatic hydrocarbons (PAH), aromatic hydrocarbons (BTEX) and mineral oils (aliphatic hydrocarbons) represent the 53% of the contaminants affecting soil and groundwater in Europe⁴¹.

Cu contamination can be attributed primarily to the discharge of industrial waste and the extensive utilization of copper sulphate (CuSO₄)-based fungicides in agricultural practices. Even if Cu is one of the seven micronutrients indispensable for plant growth, excess Cu has been identified as an important factor affecting both crop yield and quality, potentially entering the food chain. In arable land, Adrees et al. proposed 5–30 mg kg^{−1} as the optimal range of Cu soil concentration, as lower Cu concentrations result in plant deficiency, while higher levels can lead to toxic effects^{42–44}. Globally, soils are frequently subjected to multi-pollution with both inorganic and organic pollutants, which can interact and complicate risk assessment and remediation interventions⁴⁵.

Specifically, the present study focuses on testing if biochar can be effective in: (i) enhancing the biodegradation of aliphatic hydrocarbons (C10–C40), (ii) reducing the bioavailability of Cu in soil and (iii) restoring the fertility of a contaminated soil. Moreover, it aims to study if bioaugmentation and phytoremediation techniques can improve biochar potential for soil decontamination and revegetation.

In the experimental trials, a specific commercial consortium of microorganisms has been applied to a polluted soil using biochar as a carrier. Moreover, the *Melilotus officinalis* crop has been used due to its both good tolerance to organic and inorganic pollutants and its low metal translocation from roots to shoots, i.e. the phytostabilisation ability⁴⁶. Moreover, belonging to the *Leguminosae* family, *M. officinalis* has a good potential in ameliorating soil conditions by association with nitrogen fixing rhizobacteria⁴⁷. For this purpose, a series of microcosms containing soil contaminated with petroleum hydrocarbons (PHC) and Cu was set up and maintained in greenhouse for nine months. Different treatments based on biochar amendment were tested. Soil properties, microbial abundance and viability, and contaminant levels in the soil and in leaching solution were monitored during the experiment. The growth of *M. officinalis*, its photosynthetic performance and the mycorrhizal colonization of its roots were also evaluated.

Material and methods
Soil sampling and analysis

The contaminated soil was sampled in an agricultural field (northern Italy) that had been affected by oil spills from illegal pipeline tapping five years before the soil was collected. The soil was sieved at 2 mm and air-dried before chemical analysis (Table 1). Preliminary analysis showed heavy hydrocarbons contamination ($C > 12 = 10,000 \text{ mg kg}^{-1}$), above the threshold concentration set by Italian legislation for agricultural areas ($C_{10}-C_{40} = 50 \text{ mg kg}^{-1}$ as for Italian Ministry Decree DM 46/2019). In addition, before preparing the microcosms, Cu (in the form of CuSO_4) was added to the soil to reach a concentration of 250 mg kg^{-1} (above the limit of 200 mg kg^{-1} set by Italian Ministry Decree DM 46/2019).

Biochar characteristics

The biochar used in the experimental trial was produced by the Evergreen Resources s.r.l. company (Rieti, Italy) from olive and hazelnut tree pruning wastes through pyro-gasification at 850°C with a rate of 100 kg h^{-1} biomass. The biochar characteristics were reported in supplementary material (Table S1) based on a previous work³. Prior to use, the two types of biochar were mixed in a 1:1 ratio.

Experimental set-up

Eighteen microcosms were prepared and maintained in the greenhouse. Six experimental conditions in triplicate were set up using the contaminated soil as follows: (i) biochar (SB), (ii) biochar and bioactivators (SBB), (iii) biochar and plant (SBP), (iv) biochar, bioactivators, and plants (SBBP). Comparative microcosms were set up as controls using only contaminated soil without plants (S) and with plants (SP). Each microcosm consisted of an 8-L polypropylene container (Supplementary material, Fig. 2), filled with 3.57 kg of the contaminated soil (air-dried and sieved at 2 cm). An inert gravel material was placed at the bottom of each microcosm and a valve was installed to collect the leaching solution. In SB and SBP tests, biochar was thoroughly mixed with soil at a rate of 1% (w/w). In the bioaugmentation test (SBB), soil was mixed with biochar (1% w/w) plus bioactivators (0.5% w/w), e.g. a commercial consortium of microorganisms (Eurovix SpA, Italy), added according to the instructions of the manufacturer. The microbial consortium was constituted by prokaryotic cells ($3.01\text{E} + 10 \pm 4.12\text{E} + 07 \text{ N. cells g}^{-1}$) and fungi ($1.36\text{E} + 10 \pm 7.61\text{E} + 08 \text{ N. fungi g}^{-1}$) and the cell viability was 46%. Specifically, the lyophilized bioactivators powder was evenly distributed in the required volume of biochar, previously hydrated with deionized water in order to improve the adhesion of the powder to the biochar particles.

All microcosms received a nutritive solution (18 mL) containing N (2.8%), P (0.04%), K (4%) and organic C (10%) in accordance with the microorganism provider.

Melilotus officinalis L. seeds, obtained from the Fratelli Ingegnoli seed company, Milano*, were sown in SP, SBP and SBBP microcosms one month after the experimental set-up (36 seeds per microcosm). The experiment was carried out under greenhouse conditions for 9 months (March-December 2022). The mean temperature during the nine months is reported in supplementary material (Table S3). All microcosms were watered daily to replace evapotranspiration losses.

Parameter	Units	Value
Sand	g kg^{-1}	800
Silt	g kg^{-1}	113
Clay	g kg^{-1}	87
USDA textural class		SF
pH		6.4
TOC	g kg^{-1}	12.5
TN	g kg^{-1}	0.25
C/N		48.2
CEC	cm (+) kg^{-1}	3.89
P_{av}	mg kg^{-1}	4.9
K	mg kg^{-1}	1200
Ca	mg kg^{-1}	2500
Mg	mg kg^{-1}	4400
Na	mg kg^{-1}	140
Density	g cm^{-1}	1.23
Total PAH	mg kg^{-1}	12
Hydrocarbons C < 12	mg kg^{-1}	< 1.0
Hydrocarbons C10–C40	mg kg^{-1}	10.100*

Table 1. Main physico-chemical characteristics of the contaminated soil used in the experimental trial. The concentrations are expressed on the soil dry weight. *Higher than the threshold established by Italian legislation for agricultural soils ($50.0 \text{ mg kg}^{-1} \text{ dw}$; Legislative Decree 152/2006, 2006). TOC total organic carbon, TN total nitrogen, CEC cation exchange capacity, P_{av} available phosphorous.

For chemical and microbiological analyses, a representative soil sample (approx. 50 g) was collected (after mixing the soil at a depth of about 2–5 cm) from each microcosm at the beginning (T0, March) and at the end of the experiment (T9, December). In the microcosms without the plant an additional intermediate sampling (T3, June) for microbiological analysis was carried out. Non-destructive measurements on plants (estimation of leaf nitrogen and pigment content, and measurement of chlorophyll a fluorescence, see 2.6) were conducted four months after sowing (T4) and at the end of the experiment (T9). Plant biomass was determined at T9. At the same time, the leaching solution from each microcosm was collected and stored at -20°C until analysis.

Physical and chemical analysis on the soil and on the leaching solution

Contaminants

Petroleum hydrocarbons (PHC) ($\text{C} > 12$) were determined in soil and leaching solution samples. The determination of hydrocarbons ($\text{C} > 12$) was performed according to the 3550C EPA⁴⁸ and 8270D EPA⁴⁹ methods, using a GC–MS 5977B Inert Plus MSD Turbo EI Bundle—GC 8890 (Agilent, Santa Clara, CA, USA), with a column 1909 15–431 15 m and liner splitless. Hydrocarbons were extracted from soil samples using a hexane/acetone mix (1:1, v:v).

Total Cu content was determined in soil samples following the EPA 3051A method⁵⁰ and after digestion in microwave with a $\text{H}_2\text{O}_2/\text{HNO}_3$ mix (v/v, 1:2.5). For Cu fractionation, the method of the Community Bureau of Reference (BCR) (Moćko and Waćlawek, 2004) was applied. Both total Cu and fractionated Cu were determined by 5900 ICP-OES (Agilent, Santa Clara, CA; USA). Copper fractions were named: FR1; Cu fraction associated to carbonates, FR2; Cu fraction associated to Fe and Mn oxides, FR3; Cu fraction associated to organic matter, RF; Residual fraction.

To ensure the accuracy and precision of the methods, a series of quality assurance/quality control (QA/QC) procedures were performed to validate the data. Blank samples and standard reference materials (SRM) were processed along with the samples for petroleum hydrocarbons, total heavy metal and heavy metal fractionation procedures. An extraction blank was processed and analyzed with each sample set of 20. In addition, laboratory spike blank (LSB) was analyzed with each sample set of 10. The limits of quantification (LOQ) and the quality control parameters were the follows: PHC = 17.5 mg/L; Cu = 0.01 mg/L.

Soil physical and chemical analysis

Texture analysis was conducted in agreement with the procedures outlined in the Soil Survey Laboratory Methods Manual⁵¹. Soil pH was determined potentiometrically in a 1:2.5 (w/v) soil–water suspension⁵². Total Organic Carbon (TOC) and Total Nitrogen (TN) contents were determined utilising an elemental analyser (Elementar vario-MACRO cube). Available phosphorus was measured after acid extraction with 1 M NH_4F ⁵³. Soil cation exchange capacity (CEC) was determined following extraction at a pH of 8.1. Electrical conductivity (EC) was measured by a WTW multi 340i conductivity meter (Weilheim, Germany) in a 1:2.5 soil:water suspensions (w:v).

Microbial abundance and cell viability in soil

Analyses of total microbial abundance, fungal abundance (N. cells g^{-1} soil) and cell viability (% live cells/live dead) in soil were conducted using epifluorescence microscopy techniques.

Soil samples in triplicate (1 g) were transferred to a tube with 9 mL of a formaldehyde-fixed solution (130 mM NaCl; 7 mM Na_2HPO_4 , 3 mM NaH_2PO_4 ; 2% formaldehyde (v/v); 0.5% Tween 20 (v/v) and 100 mM sodium pyrophosphate) and processed as reported by Barra Caracciolo et al.⁵⁴.

Total microbial abundance (N. cells g^{-1} soil) was determined by incubating sample aliquots with 100 μL of a DAPI dye (4',6-diamidino-2-phenylindole) (1 $\mu\text{g mL}^{-1}$) for 20 min in dark condition at 4°C .

Fungal abundance (N. cells g^{-1} soil) was evaluated using the CalcoFluor White dye (Sigma-Aldrich, Germany) for detecting fungal structures in each sample⁵⁵. In particular, soil samples, fixed as described above, were stained with 20 μL of CalcoFluor White for 15 min in the dark at room temperature.

The cell viability (% live cells/live + dead) was estimated by incubating soil sample aliquots with propidium iodide and SYBR Green for detecting the live to dead cells ratio⁵⁶.

Subsequently, all soil samples stained as described above were collected on black polycarbonate filters (pore size 0.2 μm , diameter 25 mm, Millipore, Eschborn, Germany) and were placed on slides for cell average enumeration (analysing 20 fields random for each slide).

A Leica DM 4000B (Leica Microsystems, GmbH, Wetzlar, Germany) epifluorescence microscope was used for microscopy investigations.

Plant growth, physiological parameters and mycorrhizal colonisation evaluation

Nine months after sowing (T9), the plants were collected, separated into stems, leaves and roots successively weighed. To accurately remove soil particles, roots were rinsed in deionized water and air-dried before weighing. Plant material was then dried in a ventilated oven at 60°C until a stable weight was reached. Water content and dry mass were then estimated by weighting the dry samples. At T4 and T9, the chlorophyll a fluorescence transient (OJIP transients) was measured on fully expanded leaves of *Melilotus officinalis* plants through a portable fluorometer (FluorPen FP 110-LM/D, Photon System Instruments, Drasov, Czech Republic). The fluorescence measurements on leaves were performed around midday (between 10.00 a.m. and 12.00 p.m.) following 60 min of dark adaptation. A saturating light pulse of $3000 \mu\text{mol m}^{-2} \text{s}^{-1}$ was applied before each measure. The measurements were taken on 3 plants (two leaves each) per treatment. FluorPen software was used to extract data from the original measurement. The OJIP transient was analyzed through JIP test and bioenergetics parameters such as the efficiency of the water-splitting complex on the donor side (F_v/F_0) of

photosystem II (PSII), quantum yield of primary photochemistry (F_v/F_m), quantum yield of electron transport (ϕE_0) and performance index (PI_{ABS}) of PSII were determined as described by Strasser et al.⁵⁷.

Leaf nitrogen and pigment contents were estimated at T4 and T9 utilising the Dualex Scientific⁺™ (Force-A, France), a leaf clip fluorescence sensor. Measurements were made on the same leaves used for chlorophyll fluorescence measurements. The following equations were used to calculate the chlorophyll index (Eq. 1), flavonol index (Eq. 2), anthocyanin index (Eq. 3), and Nitrogen Balance Index (NBI, Eq. 4), as described by Pietrini et al.⁵⁸

$$\text{Chlorophyll index} = (T_{850} - T_{710}) / T_{710} \quad (1)$$

$$\text{Flavonol index} = \log (FRF_R / FRF_{UV}) \quad (2)$$

$$\text{Anthocyanin index} = \log (FRF_R / FRF_G) \quad (3)$$

$$\text{NBI index} = \text{Chlorophyll index} / \text{Flavonol index} \quad (4)$$

T_{850} and T_{710} are the leaf transmittance at 850 nm and 710 nm, respectively; FRF is the far-red fluorescence emission (>710 nm) excited by red (R, 650 nm), UV (UV, 375 nm), or green (G, 505 nm) light. Two Dualex readings were taken from each leaf lamina, avoiding the main veins, and then averaged to give the leaf value.

The percentage of frequency of arbuscular mycorrhizal colonization (% F) and intensity of arbuscular mycorrhizal colonization (% I) in plant roots⁵⁹ at T9 was also estimated. Dried roots were stained following the method modified from Phillips and Hayman, 1970⁶⁰. Briefly, roots were cleared with 10% KOH (w/v) for 15 min at 90 °C, then acidified at room temperature with 0.1N HCl for 1 min, and stained with 0.05% Trypan blue at 90 °C in lactic acid for 15 min. Intraradical colonization was quantified by examination of 30 randomly 1 cm-root segments, observed in groups of ten by using the Olympus BX51 microscope (200× magnification). The % F was calculated as the percentage of root segments containing hyphae, arbuscules, coils or vesicles. The % I was estimated by sorting the root segments into different intensity classes (1–20%, 21–40%, 41–60%, 61–80% and 81–100%) of intraradical coverage of arbuscular mycorrhizal (AM) typical structures.

Statistical analysis

Analyses of variance (two-way ANOVA) were performed with SigmaPlot (Version 11), (Systat Software Inc., Richmond, CA, USA) using physico-chemical soil data (e.g. pH, Pav, EC, CEC, N and C) as dependent variables, and time and remediation treatment as two independent factors. The Fisher post-hoc test was used to investigate the significance of different groups of means, considered significant at a probability level of $P < 0.05$. One-way ANOVA was carried out to assess the statistical differences among treatments for microbiological (total microbial abundance, fungal abundance and cell viability) and plant data (biomass, chlorophyll fluorescence, leaf nitrogen and pigment contents), soil Cu and PHC using the SPSS (version 26.0, Chicago, IL, United States) software tool. The statistical significance of the mean data was assessed by t-test and Tukey's Test ($p \leq 0.05$).

Analyses of the correlation between microbial abundance (Y variable) and available phosphorus content (X variable) or Cu FR3 (X variable) were performed using linear regressions with SigmaPlot (Version 11), (Systat Software Inc., Richmond, CA, USA).

For the graphical representation of the effect of the tested soil and plant variables at the initial (T0) and final (T9) time point on the experimental microcosms, two non-metric multidimensional scaling (NMDS) analyses were performed by the R package “vegan” with the dissimilarity matrix calculated by the Gower's distance. Before the NMDS analysis, the data were standardized by subtracting the mean and dividing by the standard deviation. The NMDS analyses were performed using the R Core Team, 2020 statistical software.

Results

Petroleum hydrocarbon concentration

Overall, at T9, the biochar treatments resulted in an increase in PHC removal compared to the natural attenuation process (Fig. 1a). Indeed, a reduction of 46% of the initial hydrocarbon concentration was found in S while biochar increased PHC removal from 66.7% in SB to 90% in combination with the microbial consortium (SBB). The addition of plants in the presence of the microbial consortium (SBBP) did not further increase PHC removal (88%). However, when comparing SB and SBBP, the plant stimulated the PHC reduction (from 66.7 to 88%). Chemical results of the SP microcosms are not reported because the plants did not survive until T9.

Low concentrations of hydrocarbons (mg L^{-1}) were found in the soil leachates, and they were not significantly different between treatments (Fig. 1b).

Cu concentration and bioavailability

Copper content in the soil dropped only in the treatment without biochar (14% decrease), with a correspondingly higher Cu concentration in the leaching solution although not significantly different from the other treatments (Table 2). Major variations in the Cu bioavailability pattern at T9 were reported in the SBB, SBBP, and SBBP treatments with regard to S. When biochar was applied with bioaugmentation (SBB) and phytoremediation (SBBP) treatments or with both bioaugmentation and phytoremediation (SBBP), the most bioavailable and toxic fraction, associated with carbonates (FR1) significantly decreased with respect to S, with a corresponding increase in the more recalcitrant fractions associated with Fe and Mn oxides (FR2) and to organic matter (FR3) (Fig. 2).

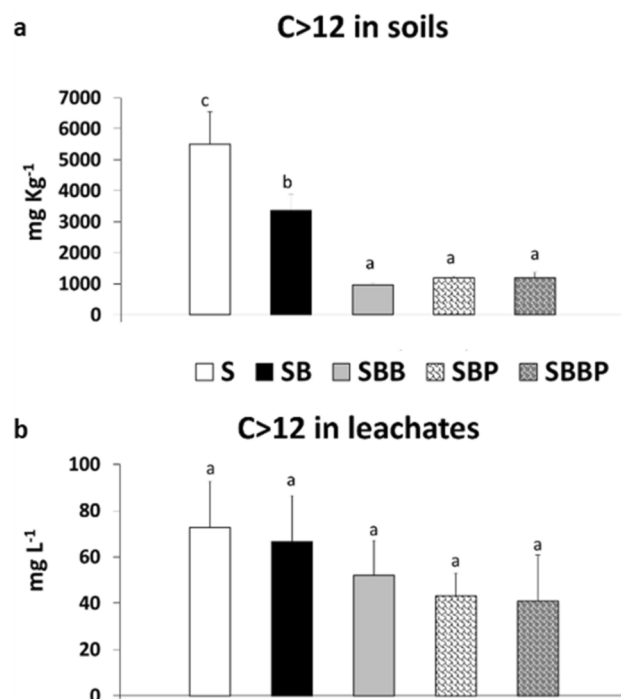


Fig. 1. Hydrocarbons C > 12 in treated soils (mg kg⁻¹ dw) (a) and in leaching solutions (b) at the end of the experiment (nine months). Treatments: contaminated soil (S), contaminated soil plus biochar (SB); contaminated soil plus biochar and bioactivators (SBB), SB plus plants (SBP), SBB plus plants (SBBP). Data are expressed as mean data ± SE (n = 3). Different letters indicate significant differences among treatments (soil and leaching solution) P < 0.05. Microsoft Excel was used to create the graphic.

Treatment	Soil Cu	Leaching Cu
S	241(± 10.1)b	1.22 (± 0.65)a
SB	260(± 13.2)ab	0.93 (± 0.20)a
SBB	280(± 24.3)a	0.92 (± 0.21)a
SBP	274(± 0.79)a	0.60 (± 0.09)a
SBBP	287(± 18.1)a	0.88 (± 0.40)a

Table 2. Total Cu in soil (mg Cu kg⁻¹ soil) and in leaching solution (mg Cu L⁻¹) at the end of the experimental period (T9). Treatments: contaminated soil (S), contaminated soil plus biochar (SB); contaminated soil plus biochar and bioactivators (SBB), SB plus plants (SBP), SBB plus plants (SBBP) (mean data ± SE; n = 3). Different letters indicate significant differences among treatments and on each matrix (soil and leaching solution) P < 0.05.

Soil chemical and physical analysis

At T0 the pH value and CEC content were significantly higher in all treated soils compared to the control (Table 3). Available phosphorus levels were also higher in the SBB treated soils than in the control soils. At T9 pH, TOC and EC showed the highest mean values in all treated soils. Conversely, significant differences were not observed in TN and CEC between treatments and control soil. In addition, the P_{av} content showed the highest values in the SBB and SBBP treated soils.

Microbial abundance and cell viability

At T0, similar total microbial abundances, with an average value of $2.26E+08 \pm 8.01E+06$ N. cells g soil⁻¹, were found (Fig. 3). In the control condition, with only contaminated soil (S), the microbial abundance remained fairly constant at T3 ($2.43E+08 \pm 6.63E+06$ N. cells g soil⁻¹; T3: $3.08E+08 \pm 3.46E+07$ N. cells g soil⁻¹) and then slightly increased at T9 ($4.75E+08 \pm 3.37E+07$ N. cells g soil⁻¹). The bioaugmentation promoted an overall increase in microbial abundance. Moreover, the combination of the biochar and bioactivator (SBB) showed the highest ($p < 0.01$) values both at T3 ($4.81E+08 \pm 2.70E+07$ N. cells g soil⁻¹) and T9 ($1.03E+09 \pm 4.21E+07$ N. cells g soil⁻¹ SBB and $8.83E+08 \pm 4.53E+07$ SBBP). On the other hand, the SB and S conditions showed the lowest microbial abundance (Fig. 3).

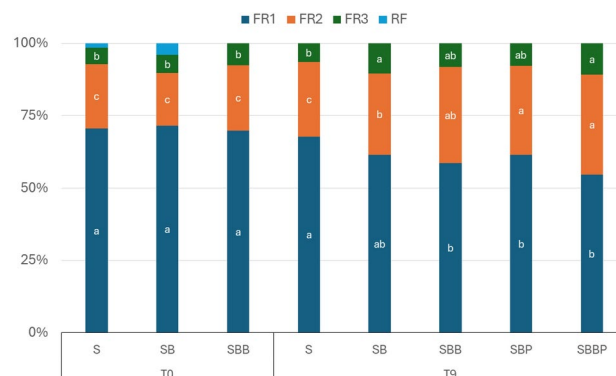


Fig. 2. Cu fractionation, in percentage at T0 (beginning) and T9 (nine months) in treated soils. Treatments: contaminated soil (S), contaminated soil plus biochar (SB); contaminated soil plus biochar and bioactivators (SBB), SB plus plants (SBP), SBB plus plants (SBBP) (mean data \pm SE; $n = 3$). FR1: Cu fraction associated with carbonates; FR2: Cu fraction associated with Fe and Mn oxides; FR3: Cu fraction associated with organic matter; RF: Residual fraction. Different letters indicate significant differences among treatments at each time $P < 0.05$. Microsoft Excel was used to create the graphic.

	S	SB	SBB	SBP	SBBP
Texture	Sandy loam				
T0					
pH	5.5 (±0.01)c	7.4 (±0.03)a	6.8 (±0.01)b	7.4 (±0.03)a	6.8 (±0.01)b
TOC %	5.14 (±0.61)a	5.54 (±1.0)a	2.24 (±0.06)b	5.54 (±1.0)a	2.24 (±0.06)b
TN %	0.05 (±0.01)b	0.05 (±0.01)b	0.09 (±0.01)a	0.05 (±0.01)b	0.09 (±0.01)a
EC (mS cm ⁻¹)	4.50 (±0.07)a	4.47(±0.09)a	4.73 (±0.09)a	4.47 (±0.09)a	4.73 (±0.09)a
CEC (cmol ₍₊₎ kg ⁻¹)	7.19 (±0.78)b	10.42 (±1.86)a	14.27 (±0.81)a	10.42 (±1.86)ab	14.27 (±0.55)a
P _{av} (mg kg ⁻¹)	34.4 (±2.8)a	36.4 (±2.3)a	52.1 (±0.8)a	36.4 (±2.3)a	52.1 (±0.8)a
T9					
pH	6.1 (±0.01)b*	7.5 (±0.03)a	7.4 (±0.03)a*	7.5 (±0.04)a	7.5 (±0.03)a*
TOC %	0.77 (±0.04)b*	1.31 (±0.07)a*	1.36 (±0.12)a*	1.46 (±0.14)a*	1.58 (±0.13)a*
TN %	0.06 (±0.02)a	0.04 (±0.00)a	0.06 (±0.02)a	0.05 (±0.00)a	0.08 (±0.01)a
EC (mS cm ⁻¹)	0.55 (±0.00)b*	0.74 (±0.04)a*	0.79 (±0.01)a*	0.67 (±0.04)a*	0.80 (±0.04)a*
CEC (cmol ₍₊₎ kg ⁻¹)	17.34 (±1.30)a*	14.22 (±0.95)a	14.01 (±1.06)a	16.51 (±0.85)a*	14.01 (±1.10)a
P _{av} (mg kg ⁻¹)	28.84 (±4.53)d	45.29 (±6.48)cd	218.8 (±36.46)a*	47.98 (±3.53)c	119.2 (±17.31)b*

Table 3. Chemical soil characteristics measured at the initial (T0) and final (T9) time points of the experiment. Treatments: contaminated soil (S), contaminated soil plus biochar (SB); contaminated soil plus biochar and bioactivators (SBB), SB plus plants (SBP), SBB plus plants (SBBP). Numbers in parentheses are the standard errors ($n = 3$). Different letters indicate significant differences among treatments and asterisks indicate significant differences between times (T0 and T9) within each treatment (two-way ANOVA analysis, $P < 0.05$). TOC total organic carbon, TN total nitrogen, EC electrical conductivity, CEC cation exchange capacity, P_{av} available phosphorous.

At T0, no significant differences among treatments in fungal abundances were observed, however an overall increase at T3 was found (Fig. 4). The significantly highest fungal abundance was found in the SBB ($3.17\text{E} + 07 \pm 3.10\text{E} + 06$ N. cells g soil^{-1}) and SB ($2.98\text{E} + 07 \pm 8.75\text{E} + 05$ N. cells g soil^{-1}) microcosms. However, at T9 fungal abundance decreased in all the experimental conditions, with average values of $7.56\text{E} + 06$ N. cells g soil^{-1} .

The microbial viability (%) at T0 indicates initial similar values (average values 33%) in all experimental conditions (Fig. 5). However, at T3, significant increases in cell viability due to biochar (SB: $71.5 \pm 3.3\%$) and bioaugmentation (SBB: $72.08 \pm 0.7\%$) were observed. However, at T9, the microbial viability generally decreased in the treated microcosms and increased in S treatment (values in the range from 28 to 50%).

Interestingly, a significant correlation was found at each time between microbial abundance and available phosphorus content ($P < 0.001$) and between microbial abundance and Cu FR3 ($P < 0.001$) (supplementary material, Fig. S4).

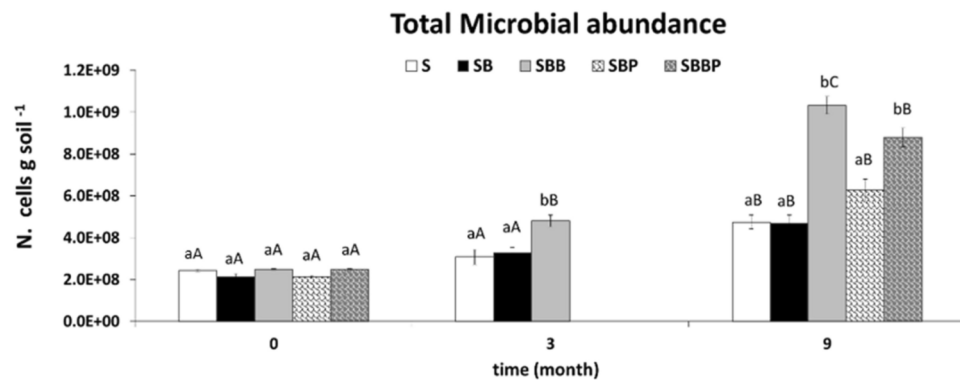


Fig. 3. Total microbial abundance (N. cells g soil⁻¹) detected by DAPI staining over the experimental time (T0, T3, T9) for all the experimental microcosms: contaminated soil (S), contaminated soil plus biochar (SB); contaminated soil plus biochar and bioactivators (SBB), SB plus plants (SBP), SBB plus plants (SBBP) (mean data \pm SE; n = 3). Different low-case letters indicate significant differences among treatments at each time (Tukey test, $P < 0.05$). Different capital letters indicate significant differences among times for each treatment (Tukey test, $P < 0.05$). Microsoft Excel was used to create the graphic.

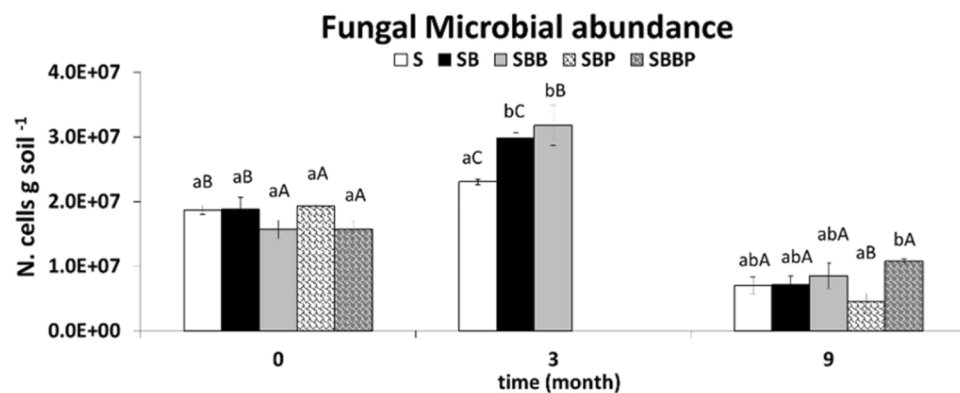


Fig. 4. Fungal Microbial abundance (N. cells g soil⁻¹) detected by CFW staining over the experimental time (T0, T3, T9) for all the experimental microcosms: contaminated soil (S), contaminated soil plus biochar (SB); contaminated soil plus biochar and bioactivators (SBB), SB plus plants (SBP), SBB plus plants (SBBP) (mean data \pm SE; n = 3). Different low-case letters indicate significant differences among treatments at each time (Tukey test, $P < 0.05$). Different capital letters indicate significant differences among times for each treatment (Tukey test, $P < 0.05$). Microsoft Excel was used to create the graphic.

Plant growth, physiological parameters, and root mycorrhizal colonisation

Plant survival rate was very low due to the intrinsic toxicity of the soil. In fact, 20 days after sowing, the seed germination rates in the SP, SBP, and SBBP microcosms were only 12%, 15%, and 15%, respectively, differing from previously tested conditions without contamination (59%)⁴⁷. However, only the plants grown in biochar presence survived until the end of the experiment (T9). Among the surviving plants, those grown with biochar and bio-activators (SBBP) showed the highest shoot height and dry biomass production (Table 4).

In order to gain insight into the potential mechanisms by which different soil treatments have affected the photosynthetic machinery in *M. officinalis* plants, the assessment of chlorophyll fluorescence parameters was carried out. At T4, when *M. officinalis* plants grown without biochar (SP) were still alive, all analysed parameters (F_v/F_m , F_v/F_0 , ϕE_0 , and PI_{ABS}) in this condition were lower than SBBP and SBP (Table 5). At T9, a different response was observed. Although higher values of ϕE_0 and PI_{ABS} were found in SBBP treated plants compared to those in SBP, no significant differences were found between treatments in the values of F_v/F_m and F_v/F_0 (Table 6). The physiological performance of *M. officinalis* plants was also evaluated by estimating the nitrogen balance index and pigment contents⁶¹. At T4, the chlorophyll and the nitrogen balance index were significantly higher in SBBP (Table 5). Moreover, data reported in Table 7 show a significant increase in anthocyanin index in plants grown without biochar (SP) compared to those treated with biochar (SBP) and biochar plus bioactivators (SBBP). At T9, as stated above, *M. officinalis* plants grown on contaminated soil (SP) did not survive. However, the chlorophyll and nitrogen balance index were significantly higher in SBBP treated plants compared to those in SBP (Table 6). The results at T9 showed that the anthocyanin index was higher in plants grown with biochar

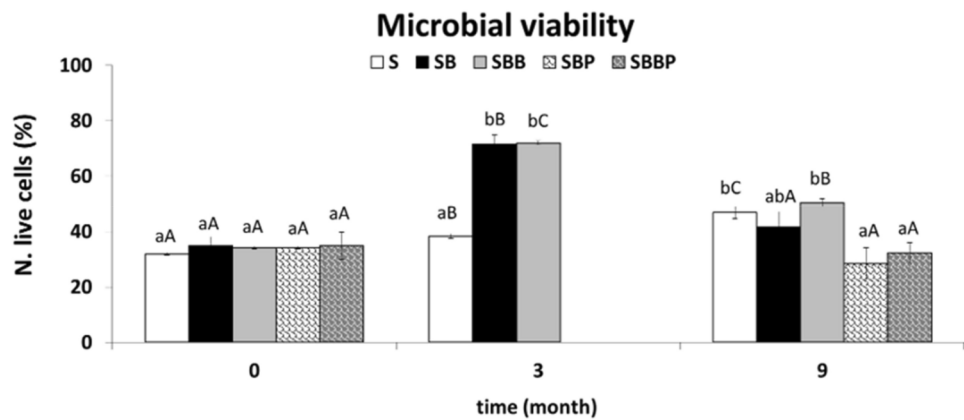


Fig. 5. Microbial viability (%) over the experimental time (T0, T3, T9) for all the experimental microcosms: contaminated soil (S), contaminated soil plus biochar (SB); contaminated soil plus biochar and bioactivators (SBB), SB plus plants (SBP), SBB plus plants (SBBP) (mean data \pm SE; n = 3). Different low-case letters indicate significant differences among treatments at each time (Tukey test, P < 0.05). Different capital letters indicate significant differences among times for each treatment (Tukey test, P < 0.05). Microsoft Excel was used to create the graphic.

Treatment	Survival rate	Shoot height	Root biomass	Aereal biomass
SP	0	–	–	–
SBP	5%	20(\pm 2.0)a	3.0(\pm 1.5)a	0.96(\pm 0.58)a
SBBP	6%	37(\pm 3.0)b	8.4(\pm 2.1)b	4.15(\pm 1.67)b

Table 4. Survival rate (%), shoot height (cm), and root and aerial dry biomass (g) measured at the end of the experimental period (T9) of plants *Melilotus officinalis* plants grown on different soil conditions: contaminated soil (SP), contaminated soil plus biochar (SBP); contaminated soil plus biochar and bioactivators (SBBP) (mean data \pm SE; n = 3). In each column, mean values with different letters differ significantly (t-test, P < 0.05).

Treatment	F_v/F_m (rel. un.)	F_v/F_0 (rel. un.)	ϕE_0 (rel. un.)	PI_{ABS} (rel. un.)
T4				
SP	0.669 (\pm 0.018)b	2.09 (\pm 0.11)b	0.265 (\pm 0.016)b	0.44 (\pm 0.05)b
SBP	0.718 (\pm 0.014)b	2.56 (\pm 0.17)b	0.327 (\pm 0.026)b	0.81 (\pm 0.16)b
SBBP	0.790 (\pm 0.004)a	3.77 (\pm 0.10)a	0.455 (\pm 0.017)a	2.47 (\pm 0.28)a

Table 5. Chlorophyll fluorescence parameters, quantum yield of primary photochemistry (F_v/F_m), efficiency of the water-splitting complex on the donor side of PSII (F_v/F_0), quantum yield of electron transport (ϕE_0) and performance index (PI_{ABS}) of photosystem II (PSII) measured four months after sowing (T4) in leaves of *Melilotus officinalis* plants grown on different soil conditions: contaminated soil (SP), contaminated soil plus biochar (SBP); contaminated soil plus biochar and bioactivators (SBBP) (mean data \pm SE; n = 6). In the columns, different letters indicate significant differences among treatments on each parameter (Tukey test, P < 0.05).

(SBP) compared to those treated with biochar plus bioactivators (SBBP). No significant differences were found in the flavonol index for each time period (Table 8).

Data about the percentage of frequency of arbuscular mycorrhizal colonization (% F) and intensity of arbuscular mycorrhizal colonization (% I) in plant roots are shown in Table 9. The % F of root colonization by AM fungi varied approximately from 39 to 50% under biochar treatments (Table 9).

Intraradical structures, such as vesicles and intraradical spores, as well as typical nodules by rhizobacteria were observed in the roots of *Melilotus* plants (supplementary material, Fig. S5).

Summarizing, the results presented above are confirmed by the non-metric multidimensional scaling analysis (NMDS). Figure 6 shows that the SBB treatment differs from the others at T0, mainly due to the values of Cu Fr3, N and Pav content. At T9, S differed from the other treatments overall based on C12 values due to likely biochar presence. Moreover, the addition of bioactivators together with biochar led to further differentiation from S. The SBB and SBBP treatments were the most different from S due to available phosphorus, DAPI, and Cu Fr3 parameters.

Treatment	F_v/F_m (rel. un.)	F_v/F_0 (rel. un.)	ϕE_0 (rel. un.)	PI_{ABS} (rel. un.)
T9				
SP	–	–	–	–
SBP	0.834 (± 0.003)a	5.06 (± 0.13)a	0.523 (± 0.003)b	5.47 (± 0.12)b
SBBP	0.840 (± 0.005)a	5.32 (± 0.20)a	0.547 (± 0.007)a	6.71 (± 0.53)a

Table 6. Chlorophyll fluorescence parameters, quantum yield of primary photochemistry (F_v/F_m), efficiency of the water-splitting complex on the donor side of PSII (F_v/F_0), quantum yield of electron transport (ϕE_0) and performance index (PI_{ABS}) of photosystem II (PSII) measured at the end of the experiment (T9) in leaves of *Melilotus officinalis* plants grown on different soil conditions: contaminated soil (SP), contaminated soil plus biochar (SBP); contaminated soil plus biochar and bioactivators (SBBP) (mean data \pm SE; n = 6). In the columns, different letters indicate significant differences among treatments on each parameter (Tukey test, $P < 0.05$).

Treatment	ChII	AntI	FlavI	NBI
T4				
SP	22.28 (± 0.57)b	0.173 (± 0.010)a	0.846 (± 0.038)a	28.01 (± 1.01)b
SBP	24.85 (± 1.93)b	0.111 (± 0.006)b	0.857 (± 0.018)a	28.71 (± 2.02)b
SBBP	34.50 (± 0.78)a	0.079 (± 0.010)b	0.915 (± 0.031)a	37.36 (± 0.65)a

Table 7. Chlorophyll index (ChII, $\mu\text{g cm}^{-2}$), anthocyanin index (AntI, abs. unit), flavonol index (FlavI, abs. unit), and nitrogen balance index (NBI, rel. un.) measured four months after sowing (T4) in leaves of *Melilotus officinalis* plants grown on different soil conditions: contaminated soil (SP), contaminated soil plus biochar (SBP); contaminated soil plus biochar and bioactivators (SBBP) (mean data \pm SE; n = 6). In the columns, different letters indicate significant differences among treatments on each parameter (Tukey test, $P < 0.05$).

Treatment	ChII	AntI	FlavI	NBI
T9				
SP	–	–	–	–
SBP	40.06 (± 1.52)b	0.078 (± 0.004)a	1.101 (± 0.07)a	36.75 (± 2.17)b
SBBP	49.62 (± 1.20)a	0.040 (± 0.008)b	1.151 (± 0.02)a	43.41 (± 2.06)a

Table 8. Chlorophyll index (ChII, $\mu\text{g cm}^{-2}$), anthocyanin index (AntI, abs. unit), flavonol index (FlavI, abs. unit), and nitrogen balance index (NBI, rel. un.) measured at the end of the experimental period (T9) in leaves of *Melilotus officinalis* plants grown on different soil conditions: contaminated soil (SP), contaminated soil plus biochar (SBP); contaminated soil plus biochar and bioactivators (SBBP) (mean data \pm SE; n = 6). In the columns, different letters indicate significant differences among treatments on each parameter (Tukey test, $P < 0.05$).

Treatment	% F	% I
SBP	39.36 (± 17.33)	55.66 (± 24.13)
SBBP	49.78 (± 6.89)	77.71 (± 3.53)

Table 9. Frequency rate (%) and Intensity rate (%) of root colonization by arbuscular mycorrhizal fungi measured at the end of the experiment (T9) of *Melilotus officinalis* plants grown on different soil conditions: contaminated soil plus biochar (SBP); contaminated soil plus biochar and bioactivators (SBBP) (mean data \pm SE; n = 3). SP colonization not evaluated.

Discussion

Soil contaminants and microbiological parameters

The degradation of PHC due to the natural attenuation processes has been described in several studies¹⁵. For example, Qin and its collaborators⁶² observed a partial hydrocarbon removal due to natural attenuation from a contaminated soil with comparable levels of PHC (16,000 mg kg⁻¹). The same authors also reported an increase (ranging from 16.6 to 23.6%) in PHC decrease after a rice straw biochar application. This result, despite the different types of biochar used, seems to be in line with our study. Following a microcosm experiment on soil samples from the same site used in the present study, Vocciante et al.⁶³ observed a downward trend in C > 12

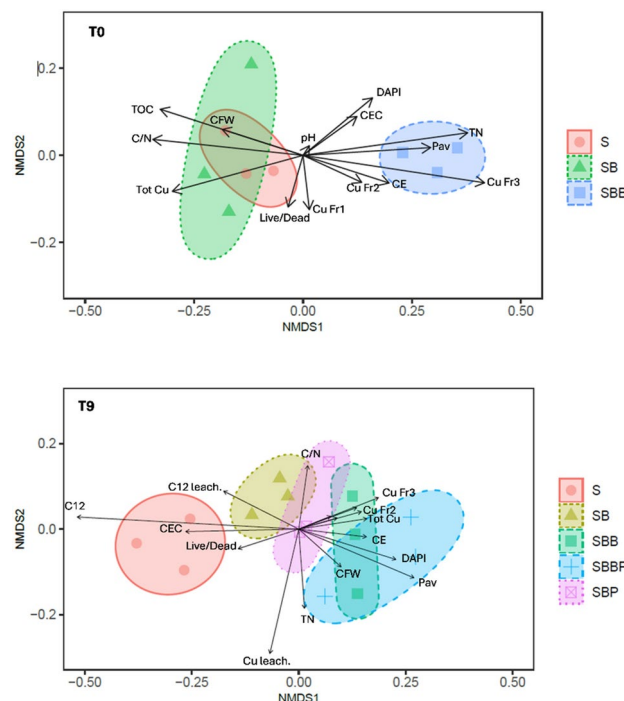


Fig. 6. The two-dimensional non-metric multidimensional scaling plots (NMDS) show the effects of the tested soil and plant variables on the experimental mesocosms at the two sampling times (T0 and T9). Treatments: contaminated soil (S), contaminated soil plus biochar (SB); contaminated soil plus biochar and bioactivators (SBB), SB plus plants (SBP), SBB plus plants (SBBP). Circle lines in NMDS plots are 95% confidence ellipses. Chemical and biochemical properties: total organic carbon, total nitrogen, total organic carbon/total nitrogen ratio, total Cu concentration, cation exchange capacity, total microbial abundance, electrical conductivity, available phosphorous, Cu fraction associated to carbonates, Cu fraction associated to Fe and Mn oxides, Cu fraction associated to organic matter, C > 12 in soils, C > 12 in leaching solutions, total Cu in leaching solutions. R software environment was used to create the graphic.

hydrocarbons after 1 month of testing, which appeared to be further favored by the presence of plants. Moreover, in accordance with our results (Fig. 1), other studies showed that, when a bioaugmentation strategy was applied in combination with biochar, the biodegradation of PHC increased^{18,37}. In this regard, Mukome et al.⁶⁴, in a study on the degradation of light and heavy crude oils in soil added with pine wood biochar, highlighted the importance of nutrient availability for soil microorganisms to increase the efficiency of the of heavy hydrocarbon degradation. In the present study (Fig. 3a), the highest PHC degradation observed in SBB was presumably associated with the highest microbial abundance and in particular the bioaugmented microorganisms specialized in hydrocarbon removal⁶⁵. In fact, an increase in fungi was observed in the microcosms with biochar (T3) suggesting possible support for fungal strains in the degradation of hydrocarbons during the experimental timespan (Fig. 4), as reported in other studies dealing with PHC degradation in soil^{66–68}. Moreover, the lack of significant differences among treatments in PHC content of the leaching solutions, confirms that their reduction in the microcosms was due to soil degradation processes (Fig. 3b). Mukherjee et al.¹¹ ascribed the biochar-induced hydrocarbon degradation to the following mechanisms: (i) the electron transfer ability of biochar surfaces that can promote redox-active reactions, (ii) the influence on the microbial habitat exerted by the presence of free radicals and reactive oxygen species on biochar through the supply of surface adsorbed nutrients and energy.

In our study, the presence of biochar led to an increase in the most stable Cu fraction (Fig. 2). In addition, the biochar amendment together with bioaugmentation and/or phytoremediation resulted in a further decrease in the most bioavailable Cu fraction. In this context, Zafeiriou et al.⁶⁹ reported a decrease in the acid soluble fraction of Cu in soils amended with sewage sludge derived biochar compared to the control. Moreover, the oxidizable Cu fraction was noticeably increased in biochar amended soils, compared with the controls. These authors attributed this response to the liming effect of biochar when it is applied to an acid soil, rising its pH⁷⁰. In our case, adding biochar increased soil pH from 6.1 to 7.5. A higher pH enhances Cu hydrolysis and favors the formation of metal cations complexes by soil components⁶⁹ and on the biochar particles themselves⁷¹, reducing Cu availability. The immobilisation and stabilisation of Cu can be also achieved by its interaction with biochar through metal exchange and complexation with various functional groups on biochar.

The treatment with biochar, plants, and bioactivators (SBBP) resulted in the lowest bioavailable and toxic fraction of Cu associated with carbonates compared to the other treatments. This can be due to root exudates which can induce changes in Cu fractionation through the pH alteration, provision of ligands for its complexation, and facilitation of microbial activity⁷². In our case, no pH changes have been observed in plant presence (Table 3), therefore root exudates might have acted as natural chelates, forming complexes in the rhizosphere⁷³. For

example, low molecular weight organic acids, are reported to form stable extracellular complexes with Cu⁷⁴. Moreover, rhizosphere bacteria can have different levels of tolerance to different heavy metals. Microorganisms can use various mechanisms to remediate soil and water contaminated with heavy metals and can support plants to tolerate stress and boost plant growth and productivity. These mechanisms include biosorption, secreting extracellular barriers, bioaccumulation, actively transporting metal ions, producing metal chelators, and detoxifying through enzymes^{75,76}. In particular, phosphate solubilising bacteria are commonly used for heavy metal remediation⁷⁷. Phosphate-solubilising bacteria in soil have the capacity to convert insoluble phosphorus forms into phosphate ions, which can then react with heavy metal ions to form metal phosphate precipitates with very low solubility⁷⁸. The higher available phosphorus content found in treatments with bioactivators (Table 3) could be associated with the presence of this kind of microorganisms. In this regard, a significant correlation between available phosphorus values and microbial abundance has been found (supplementary material, Fig. S4). Other authors have also shown that microorganisms together with biochar may reduce metal bioavailability. Tu et al.²¹ found that application of biochar with *Pseudomonas* NT-2 reduced the proportion of soil-exchangeable Cd and carbonate-bound Cu by 12.82% and 26.55% respectively, thereby decreasing plant availability of heavy metals. In another work, Lai et al.⁷⁹ showed that the combination of biochar and phosphate solubilizing microorganisms remediated Pb and Cd mixed pollution from soil, mainly through formation of Pb phosphate and Cd carbonate. In our case, it is noticeable the correlation found between microbial abundance and Cu bound to Fe and Mn oxides at all time intervals (supplementary material, Fig. S4).

Microbiological results show how a microbial population able to tolerate and potentially remove the high PHC and Cu contamination was already present in the studied soil (Figs. 3, 4, 5). In fact, with the natural attenuation process of PHC in S microcosms (Fig. 1), a relative increase in microbial abundance was also observed. Indeed, natural soil microbial populations can adapt to survive in a contaminated and nutrient-poor environment^{80,81} and develop degradation capabilities⁸². Petroleum hydrocarbons can stimulate microbial populations to decompose or tolerate hydrocarbons⁸³. In our study, in the time span between the oil spill event and our experiment (5 years), a selection of PHC adapted microbial populations could be occurred, although their attenuation capabilities were quite slow. The combination of biochar and bioactivators (SBB) enhanced microbial abundance. In fact, the porous structure of biochar facilitates the formation of both aerobic and anaerobic microhabitats, providing the nutrients and energy necessary for microbial colonization. Because PHC removal requires both aerobic and anaerobic processes for their degradation¹⁵, biochar, among other advantages, can promote their removal. Additionally, the high surface area and adsorption capacity of biochar enable it to immobilize toxic compounds, such as heavy metals, while promoting the growth and reproduction of microorganisms^{11,14,23,84,85}. At T9 the microbial viability generally decreased in the treated microcosms and increased in S treatment, presumably due to a selection of different bacterial populations depending on the conditions.

Germination, plant growth and root mycorrhizal colonization

The addition of the biochar amendment (SB) and biochar amendment plus bioactivators (SBB) to the contaminated soil had a beneficial effect on the growth and physiological performance of *Melilotus officinalis* plants. The positive impact of these treatments was appreciable from the seed germination phase. Seeds sown in SB and SBB had a higher germination rate (15%) compared to those in SP microcosms (12%) after 20 days from sowing. Oh et al.⁸⁶ found similar results, indicating that aqueous extracts of different biochar samples increased the rate of germination and seedling growth of lettuce seeds compared to the control group. Consistently, at T9, the root and aerial biomass of *Melilotus officinalis* plants in both SBP and SBBP microcosms were healthy, differently from SP where the plants did not survive (Table 4) owing to higher hydrocarbon persistence, Cu bioavailability and their associated toxicity¹⁵. Indeed, hydrocarbons can hamper the transfer of water and oxygen through sediment and soil pores, preventing vegetation development¹⁵.

These results can be ascribed to organic carbon and nutrients added to the soil through the biochar which were absorbed by plants, enhancing their development^{87,88}. Furthermore, biochar inducing changes in nutrient availability, provide also additional sources of N, P and C to root-associated microorganisms⁸⁹. Several studies have in fact reported an improvement in plant-associated microbial activity in soil amended with biochar for different crops^{90,91}.

The outcomes of the present study show that plants grown in SBBP microcosms had the best growth performance, highlighting the effectiveness of the combination of biochar and bioactivators in enhancing the growth and development of the *Melilotus officinalis* plants (Table 4). This finding is in agreement with the results reported by Ma et al.⁹², who evaluated the growth of lettuce plants after applying three types of biochar to soil, both individually and in combination with plant-beneficial microbes.

Moreover, the higher biomass of SBBP plants with regards to SBP plants may be related with the higher soil available phosphorus content (Table 3). The available phosphorus can be absorbed and utilised by plants through their own metabolism. Phosphate solubilising microorganisms have also been demonstrated to enhance plant uptake of elements such as nitrogen, potassium and calcium, and as a consequence also plant growth and development⁹³. Furthermore, they have the capacity to deliver the auxin indole-3-acetic acid, gibberellic acid and cytokinin to enhance plant root growth. In general terms, biochar has been demonstrated to enhance soil nutrients, thereby stimulating root growth. A recent meta-analysis of scientific literature has indicated a positive correlation between the increase in root biomass in the presence of biochar and TOC, TN and P_{av}⁹⁴.

Finally, the slightly higher percentage of frequency of arbuscular mycorrhizal colonization (% F) and intensity of arbuscular mycorrhizal colonization (% I) in SBBP roots compared to SBP ones could be attributed to the microbial component present in the SBBP treatment (Table 9). Mycorrhizal symbiosis is generally altered by the presence of soil microorganisms, in particular, bacteria in the rhizosphere, and soil P availability^{95,96}. The available phosphorus content in SBB and SBBP treatments (higher in SBBP) may suggest the presence of certain bacterial species capable of solubilizing phosphate into an accessible form, facilitating the absorption and translocation to

the plant, and consequently, may stimulate AM fungal root colonization and promote plant growth. Regarding the typical intraradical structures of *Glomeraceae* family observed in roots of *Melilotus* plants, it is widely documented that autochthonous AM fungal species from this family are found in hydrocarbon polluted soils, showing a notable adaptability and tolerance performance against these stressful abiotic conditions⁹⁷.

Evaluation of plant physiological parameters

To investigate the physiological response of *Melilotus officinalis* plants to the different treatments, the chlorophyll fluorescence analyses including JIP-test were conducted. Chlorophyll fluorescence parameters serve as pivotal indicators of photosynthetic and physiological processes, offering valuable insights into the relationship between plants and their environment^{29,98}. As detailed in the results section, four months after sowing (T4), all chlorophyll fluorescence parameters were significantly higher in *Melilotus officinalis* plants grown in SBBP microcosms in comparison to those grown in SP and SBP (Table 5). In particular, plants grown in SP microcosms exhibited F_v/F_m values that were lower than the range of 0.7–0.8, which is commonly reported for healthy leaves^{99,100}. The lower values of F_v/F_m observed in SP microcosms indicate that a proportion of the PSII reaction centre is damaged or inactivated, a phenomenon generally associated to plants under stress conditions¹⁰¹. Furthermore, the efficiency of the water-splitting complex on the donor side of PSII (F_v/F_0) exhibited a similar pattern to that observed for F_v/F_m (Table 5). The F_v/F_0 ratio is also supposed to indicate with more sensitivity and higher amplitude the effects of potential photoinhibition than F_v/F_m ¹⁰². In our study, the decreased F_v/F_0 ratio observed in SP plants indicates a reduced efficiency of the water-splitting complex on the donor side of PSII¹⁰³. This suggests the involvement of a donor side photoinhibition mechanism, possibly due to malfunction of the water-splitting complex, which may result in the formation of harmful oxidations in PSII^{104,105}. These results were confirmed by the similar trend observed for the quantum yield of electron transport (ϕE_0) and the performance index (PI_{ABS}). In particular, the decrease in the performance index (PI_{ABS}), which is considered more sensitive to environmental effects than the generally used parameter F_v/F_m and presents a good correlation with photosynthetic capacity, as determined by CO_2 assimilation^{106,107}, indicated a low photosynthetic efficiency in plants grown in SP microcosms. Progressive damage to the photosynthetic apparatus probably due to the soil contamination caused the death of plants grown in SP microcosm 5 months after sowing (T5). Four months after sowing (T4), the plants grown in SBP microcosms also exhibited values of chlorophyll fluorescence parameters that were lower than those observed in *Melilotus officinalis* plants grown in SBBP microcosms (Table 5). However, the values of F_v/F_m in SBP plants remained within the range of 0.7–0.8, indicating that the energy levels were sufficient to drive photosynthetic reactions⁹⁹. The capacity of plants grown in SBP microcosms to maintain a relatively high efficiency of the photosynthetic apparatus enabled them to partially recover the gap with plants grown in SBBP at T9. The findings obtained align with those previously reported by Fedeli et al.¹⁰⁸, in which the incorporation of biochar into contaminated soils demonstrated a favourable impact on the growth of *Avena sativa* L. plants, reducing the detrimental impacts provoked by gasoline on all the eco-physiological parameters under consideration. Regarding the plants grown in SBBP microcosms, the results showed that they exhibited the best physiological performance at both four (T4) and nine (T9) months after sowing. In detail, the quantum yield of primary photochemistry (F_v/F_m), the efficiency of the water-splitting complex on the donor side of PSII (F_v/F_0) and the electron transport to beyond Q_A (ϕE_0) were increased by the application of the combination of biochar and bioactivators. This indicated that the transport of electrons from the reaction centre (RC) to the plastoquinone (PQ) pool was promoted. Similarly, the performance index (PI_{ABS}) was also enhanced in biochar plus bioactivators treatments (Tables 5 and 6). These data indicated that the normal energy fluxes, the quantum yields and efficiencies beyond Q_A (F_v/F_m and ϕE_0) of *Melilotus officinalis* leaves could be effectively maintained by an addition of biochar and bioactivators to the contaminated soil. The results obtained in this experiment are in accordance with those previously reported by Rajput et al.¹⁰⁹, in which the addition of a biochar amendment with bacteria to polluted soils was found to enhance the photosynthetic activity of *Hordeum vulgare* L. plants when compared to the individual application of bacteria and biochar.

The physiological performance of *M. officinalis* plants was also evaluated through the estimation of the pigment contents and the nitrogen balance index. These parameters offer insights into the physiological status of plants, as well as their photosynthetic potential and primary production⁹. As reported in the results section, four months after sowing (T4), chlorophyll and nitrogen balance index were significantly higher in *Melilotus officinalis* plants grown in SBBP microcosms in comparison to those grown in SP and SBP. In contrast, anthocyanin index was higher in plants grown in SP microcosms with respect to the other treatments (Table 7). Furthermore, no statistically significant differences in the flavonol index among treatments were observed (Table 7). The results of chlorophyll and nitrogen balance index are in conformity with those observed in chlorophyll fluorescence data, in which the lowest values were found in plants grown in SP microcosms. The observed decline in chlorophyll content in SP plants is corroborated by numerous studies that have documented analogous reductions resulting from soil contamination with petroleum and its derivatives^{110–112}. Furthermore, the similar decreasing trend observed in the nitrogen balance index may be attributable to the well-documented correlation between chlorophyll and leaf nitrogen content^{113,114}. Anthocyanins and flavonols are two classes of flavonoids that occur naturally in plants. They have a role in the defense of plants from a diverse array of environmental stresses^{115,116}. In the context of this study, an increase in the anthocyanin index could be attributed to the stress condition experienced by plants grown in SP microcosms due to the persistence of hydrocarbon contamination. Similar findings were reported by Heidari et al.¹¹⁷, who observed that plants of *Echinacea purpurea* exposed to different concentrations of crude oil exhibited a significant increase in anthocyanin content and a notable reduction in chlorophyll content. As previously reported, the progressive damage to the photosynthetic apparatus, likely due to soil contamination, resulted in the death of plants grown in the SP microcosm nine months after sowing (T9). Four months after sowing (T4), the plants grown in SBP microcosms also exhibited values of chlorophyll and nitrogen balance index that were lower than those observed in *Melilotus officinalis* plants grown in SBBP

microcosms (Table 7), where hydrocarbons were almost removed, and their toxicity reduced significantly. Nevertheless, as previously stated, the ability of plants grown in SPB microcosms to sustain a relatively high photosynthetic efficiency, coupled with a quite good chlorophyll content, enabled them to partially recover the deficit with plants grown in SBBP microcosms at the end of the experiment (T9, Table 8). Indeed, as reported in the literature, the biochar-treated soil provides a favorable environment for plant growth of willow and maize, significantly reducing the toxicity and bioavailability of contaminants^{27,118}. In fact, adding biochar to soils contaminated with heavy metals can reduce their toxicity to plants, promoting plant growth and limiting the entry of heavy metals into the food chain³³. In our study, the reduction of the toxicity of the contaminants in plants grown in SBP microcosms was also confirmed by the low values of the anthocyanin index (Tables 7 and 8). This condition was more pronounced in plants grown in SBBP microcosms, which exhibited the highest values of chlorophyll and nitrogen balance index and the lowest values of anthocyanin index at both four (T4) and nine (T9) months after sowing (Tables 7 and 8). The results of our study are in agreement with those reported by Zhang et al.²³, which indicated that integrated applications of biochar and bioaugmented microbes may enhance soil organic carbon contents and other physicochemical characteristics, thereby promoting plant growth and productivity in contaminated soil.

Conclusions

The natural attenuation of PHC observed in the contaminated soil shows the presence of autochthonous microbial populations able to degrade partially petroleum hydrocarbons over the experimental time (range $2.43\text{E}+08$ – $4.75\text{E}+08$ N. cells g soil⁻¹). However, the biochar amendment improved significantly hydrocarbon removal (from 46% of S to 66.7% of SB) and promoted a partial immobilization of copper, allowing plants to survive in the contaminated soil and increase their tolerance to stress. The combined action of the biochar with bioaugmentation (SBB) and/or phytoremediation (SBP; SBBP) promoted a further decrease of PHC from soil (arriving at 88–90%). This effect can be ascribed to the highest microbial abundances due to the combined action of biochar, bioactivators and/or plant roots which promoted directly and indirectly degradative microbial activity (in the range from $6.25\text{E}+08$ to $1.03\text{E}+09$ N. cells g soil⁻¹ at T9). The combination of bioactivators and biochar (SBBP) was the most effective in promoting *M. officinalis* growth, as evidenced by plant biomass (three-fold higher in SBBP than SBP) and by physiological parameters. To ensure successful revegetation of hydrocarbon-contaminated soil, applying this plant species with biochar and bioactivators is recommended. Results of this work can be useful in future brownfield revegetation/remediation programs. Finally, it is worth mentioning that, in the long term, plants can further enhance ecological interactions among soil microbial populations and provide further hydrocarbon removal, as well as other valuable ecosystem services.

Data availability

The data that support the findings of this study are available from the corresponding author upon request.

Received: 28 November 2024; Accepted: 10 March 2025

Published online: 02 April 2025

References

- Seow, Y. X. et al. A review on biochar production from different biomass wastes by recent carbonization technologies and its sustainable applications. *J. Environ. Chem. Eng.* **10**, 107017 (2022).
- Ayaz, M. et al. Biochar role in the sustainability of agriculture and environment. *Sustainability* **13**, 1330 (2021).
- Massaccesi, L. et al. Short-term effects of biochar and compost on soil microbial community, C and N cycling, and lettuce (*Lactuca sativa* L.) yield in a Mediterranean environment. *Appl. Soil Ecol.* **199**, 105411 (2024).
- Nogués, I. et al. Biochar soil amendment as carbon farming practice in a Mediterranean environment. *Geoderma Region.* **33**, e00634 (2023).
- Gholizadeh, M. & Hu, X. Removal of heavy metals from soil with biochar composite: A critical review of the mechanism. *J. Environ. Chem. Eng.* **9**, 105830 (2021).
- Palmegiani, G., Lebrun, M., Simiele, M., Bourgerie, S. & Morabito, D. Effect of biochar application depth on a former mine technosol: impact on metal (loid)s and *Alnus* growth. *Environments* **8**, 120 (2021).
- Sun, Y., Wang, T., Bai, L., Han, C. & Sun, X. Application of biochar-based materials for remediation of arsenic contaminated soil and water: Preparation, modification, and mechanisms. *J. Environ. Chem. Eng.* **10**, 108292 (2022).
- Wu, Y., Yan, Y., Wang, Z., Tan, Z. & Zhou, T. Biochar application for the remediation of soil contaminated with potentially toxic elements: Current situation and challenges. *J. Environ. Manag.* **351**, 119775 (2024).
- Dai, Y. et al. Effects of shade treatments on the photosynthetic capacity, chlorophyll fluorescence, and chlorophyll content of *Tetrastigma hemsleyanum* Diels et Gilg. *Environ. Exp. Bot.* **65**, 177–182 (2009).
- Zhang, F., Liu, M., Li, Y., Che, Y. & Xiao, Y. Effects of arbuscular mycorrhizal fungi, biochar and cadmium on the yield and element uptake of *Medicago sativa*. *Sci. Total Environ.* **655**, 1150–1158 (2019).
- Mukherjee, S. et al. Biochar-microorganism interactions for organic pollutant remediation: Challenges and perspectives. *Environ. Pollut.* **308**, 119609 (2022).
- Zhang, W. Influence of alpine meadow deterioration on soil microbial communities in the Yangtze River source region. *Front. Environ. Sci.* **11**, 1210349 (2023).
- Xu, X. et al. Petroleum hydrocarbon-degrading bacteria for the remediation of oil pollution under aerobic conditions: a perspective analysis. *Front. Microbiol.* **9**, 2885 (2018).
- Sui, X., Wang, X., Li, Y. & Ji, H. Remediation of petroleum-contaminated soils with microbial and microbial combined methods: Advances, mechanisms, and challenges. *Sustainability* **13**, 9267 (2021).
- Pandolfo, E., Barra Caracciolo, A. & Rolando, L. Recent advances in bacterial degradation of hydrocarbons. *Water* **15**, 375 (2023).
- Ferraro, A. et al. Bioaugmentation strategy to enhance polycyclic aromatic hydrocarbons anaerobic biodegradation in contaminated soils. *Chemosphere* **275**, 130091 (2021).
- Chen, H. et al. Evaluating the protection of bacteria from extreme Cd (II) stress by P-enriched biochar. *Environ. Pollut.* **263**, 114483 (2020).

18. Dike, C. C. et al. The co-application of biochar with bioremediation for the removal of petroleum hydrocarbons from contaminated soil. *Sci. Total Environ.* **849**, 157753 (2022).
19. Guan, R. et al. The mechanism of DEHP degradation by the combined action of biochar and *Arthrobacter* sp. JQ-1: Mechanisms insight from bacteria viability, degradation efficiency and changes in extracellular environment. *Chemosphere* **341**, 140093 (2023).
20. Manikandan, S. K. et al. Effective usage of biochar and microorganisms for the removal of heavy metal ions and pesticides. *Molecules* **28**, 719 (2023).
21. Tu, C. et al. Biochar and bacteria inoculated biochar enhanced Cd and Cu immobilization and enzymatic activity in a polluted soil. *Environ. Int.* **137**, 105576 (2020).
22. Wei, X. et al. In *IOP Conference Series: Earth and Environmental Science*. 012096 (IOP Publishing).
23. Zhang, B., Zhang, L. & Zhang, X. Bioremediation of petroleum hydrocarbon-contaminated soil by petroleum-degrading bacteria immobilized on biochar. *RSC Adv.* **9**, 35304–35311 (2019).
24. Qi, Y., Liu, H., Wang, J. & Wang, Y. Effects of different straw biochar combined with microbial inoculants on soil environment in pot experiment. *Sci. Rep.* **11**, 14685 (2021).
25. Rawat, J., Sanwal, P., Saxena, J. & Prasad, R. Exploring the biochar as a suitable carrier for a bioinoculant *Aspergillus niger* K7 and its consequence on *Eleusine coracana* in field studies. *J. Agric. Food Res.* **14**, 100825 (2023).
26. Ajeng, A. A. et al. Bioformulation of biochar as a potential inoculant carrier for sustainable agriculture. *Environ. Technol. Innov.* **20**, 101168 (2020).
27. Lebrun, M. et al. Effects of carbon-based materials and redmuds on metal (loid) immobilization and growth of *Salix dasyclados* Wimm. on a former mine technosol contaminated by arsenic and lead. *Land Degrad. Dev.* **32**, 467–481 (2021).
28. Bolan, S. et al. The potential of biochar as a microbial carrier for agricultural and environmental applications. *Sci. Total Environ.* **886**, 163968 (2023).
29. Pietrini, F. et al. Morpho-physiological and metal accumulation responses of hemp plants (*Cannabis sativa* L.) grown on soil from an agro-industrial contaminated area. *Water* **11**, 808 (2019).
30. Vidali, M. Bioremediation. An overview. *Pure Appl. Chem.* **73**, 1163–1172 (2001).
31. Pulford, I. D. & Watson, C. Phytoremediation of heavy metal-contaminated land by trees—a review. *Environ. Int.* **29**, 529–540 (2003).
32. Mench, M., Vangronsveld, J., Clijsters, H., Lepp, N. & Edwards, R. In *Phytoremediation of Contaminated Soil and Water* 323–358 (CRC Press, 2020).
33. Ren, W.-L., Ullah, A. & Yu, X.-Z. Biochar influences phytoremediation of heavy metals in contaminated soils: an overview and perspectives. *Environ. Sci. Pollut. Res.* 1–29 (2024).
34. Caracciolo, A. B. et al. Changes in microbial community structure and functioning of a semiarid soil due to the use of anaerobic digestate derived composts and rosemary plants. *Geoderma* **245**, 89–97 (2015).
35. Ghosh, D. & Maiti, S. K. Can biochar reclaim coal mine spoil? *J. Environ. Manag.* **272**, 111097 (2020).
36. Guirado, M. et al. Effectiveness of biochar application and bioaugmentation techniques for the remediation of freshly and aged diesel-polluted soils. *Int. Biodeterior. Biodegrad.* **163**, 105259 (2021).
37. Guo, M., Song, W. & Tian, J. Biochar-facilitated soil remediation: mechanisms and efficacy variations. *Front. Environ. Sci.* **8**, 521512 (2020).
38. Picariello, E., Baldantoni, D. & De Nicola, F. How soil microbial communities from industrial and natural ecosystems respond to contamination by polycyclic aromatic hydrocarbons. *Processes* **11**, 130 (2023).
39. Yan, A. et al. Phytoremediation: a promising approach for revegetation of heavy metal-polluted land. *Front. Plant Sci.* **11**, 359 (2020).
40. Xiang, L. et al. Integrating biochar, bacteria, and plants for sustainable remediation of soils contaminated with organic pollutants. *Environ. Sci. Technol.* **56**, 16546–16566 (2022).
41. Baritz, R. et al. Soil monitoring in Europe—Indicators and thresholds for soil health assessments. *EEA Re. Publ. Off. Eur. Union.* **8** (2023).
42. Adrees, M. et al. The effect of excess copper on growth and physiology of important food crops: a review. *Environ. Sci. Pollut. Res.* **22**, 8148–8162 (2015).
43. Ballabio, C. et al. Copper distribution in European topsoils: An assessment based on LUCAS soil survey. *Sci. Total Environ.* **636**, 282–298 (2018).
44. Wang, Y., Chen, X. & Chen, J. Advances of the mechanism for copper tolerance in plants. *Plant Sci.* 112299 (2024).
45. Ndour, P. M. S., Langrand, J., Fontaine, J. & Lounès-Hadj Sahraoui, A. Exploring the significance of different amendments to improve phytoremediation efficiency: focus on soil ecosystem services. *Environ. Sci. Pollut. Res.* 1–29 (2024).
46. Steliga, T. & Kluk, D. Assessment of the suitability of *Melilotus officinalis* for phytoremediation of soil contaminated with petroleum hydrocarbons (TPH and PAH), Zn, Pb and Cd based on toxicological tests. *Toxics* **9**, 148 (2021).
47. Nogues, I. et al. Cultivation of *Melilotus officinalis* as a source of bioactive compounds in association with soil recovery practices. *Front. Plant Sci.* **14**, 1218594 (2023).
48. (EPA), U. E. P. A. Method 3550C: ultrasonic extraction, part of test methods for evaluating solid waste Physical/chemical methods 17 (2007).
49. (EPA), U. E. P. A. Method 8270D. Semivolatile organic compounds by gas chromatography mass spectrometry. 71 (2007).
50. (EPA), U. E. P. A. Method 3051A: Microwave assisted acid digestion of sediments, sludges, soils, and oils. 30 (2007).
51. Service, U. S. D. o. A. N. R. C. Kellogg Soil Survey Laboratory Methods Manual. Soil Survey Investigations Report No. 42 Version 5.0. (2014).
52. LP, V. R. Procedures for soil analysis, 6th edition. (*No Title*). **119** (2002).
53. Bray, R. H. & Kurtz, L. T. Determination of total, organic, and available forms of phosphorus in soils. *Soil Sci.* **59**, 39–46 (1945).
54. Caracciolo, A. B. et al. Effect of urea on degradation of terbutylazine in soil. *Environ. Toxicol. Chem. Int. J.* **24**, 1035–1040 (2005).
55. Policastro, G., Ferraro, A., Miritana, V. M., Massini, G. & Fabbicino, M. Fermentative hydrogen production enhancement by microbial community selection and enrichment through biostimulation. *Fuel* **355**, 129396 (2024).
56. Grenni, P. et al. Effects of wood amendments on the degradation of terbutylazine and on soil microbial community activity in a clay loam soil. *Water Air Soil Pollut.* **223**, 5401–5412 (2012).
57. Strasser, R. J., Tsimilli-Michael, M. & Srivastava, A. In *Chlorophyll a Fluorescence: A Signature of Photosynthesis* 321–362 (Springer, 2004).
58. Pietrini, F., Passatore, L., Carloni, S. & Zacchini, M. In *Emerging Contaminants and Plants: Interactions, Adaptations and Remediation Technologies* 87–108 (Springer, 2023).
59. Declerck, S., D'Or, D., Bivort, C. & de Souza, F. A. Development of extraradical mycelium of *Scutellopora reticulata* under root-organ culture: spore production and function of auxiliary cells. *Mycol. Res.* **108**, 84–92 (2004).
60. Phillips, J. & Hayman, D. Improved procedures for clearing roots and staining parasitic and vesicular-arbuscular mycorrhizal fungi for rapid assessment of infection. *Trans. Br. Mycol. Soc.* **55**, 158–IN118 (1970).
61. da Silva, J. M., Fontes, P. C. R., Milagres, C. d. C. & Garcia Junior, E. Application of proximal optical sensors to assess nitrogen status and yield of bell pepper grown in slab. *J. Soil Sci. Plant Nutr.* **21**, 229–237 (2021).
62. Qin, G., Gong, D. & Fan, M.-Y. Bioremediation of petroleum-contaminated soil by biostimulation amended with biochar. *Int. Biodeterior. Biodegrad.* **85**, 150–155 (2013).

63. Vocciant, M. et al. Sustainable recovery of an agricultural area impacted by an oil spill using enhanced phytoremediation. *Appl. Sci.* **14**, 582 (2024).
64. Mukome, F. N. et al. Biochar amendment as a remediation strategy for surface soils impacted by crude oil. *Environ. Pollut.* **265**, 115006 (2020).
65. Vasudevan, V., Gayathri, K. V. & Krishnan, M. E. G. Bioremediation of a pentacyclic PAH, Dibenz (a, h) Anthracene-A long road to trip with bacteria, fungi, autotrophic eukaryotes and surprises. *Chemosphere* **202**, 387–399 (2018).
66. Madadi, R. & Bester, K. Fungi and biochar applications in bioremediation of organic micropollutants from aquatic media. *Mar. Pollut. Bull.* **166**, 112247 (2021).
67. Quilliam, R. S., Glanville, H. C., Wade, S. C. & Jones, D. L. Life in the 'charosphere'—Does biochar in agricultural soil provide a significant habitat for microorganisms? *Soil Biol. Biochem.* **65**, 287–293 (2013).
68. García-Delgado, C., Alfaro-Barta, I. & Eymar, E. Combination of biochar amendment and mycoremediation for polycyclic aromatic hydrocarbons immobilization and biodegradation in creosote-contaminated soil. *J. Hazard. Mater.* **285**, 259–266 (2015).
69. Zafeiriou, I. et al. Effects of biochars derived from sewage sludge and olive tree prunings on Cu fractionation and mobility in vineyard soils over time. *Land* **12**, 416 (2023).
70. Hass, A. et al. Chicken manure biochar as liming and nutrient source for acid Appalachian soil. *J. Environ. Qual.* **41**, 1096–1106 (2012).
71. Egene, C. E., Van Poucke, R., Ok, Y. S., Meers, E. & Tack, F. Impact of organic amendments (biochar, compost and peat) on Cd and Zn mobility and solubility in contaminated soil of the Campine region after three years. *Sci. Total Environ.* **626**, 195–202 (2018).
72. Gobran, G. R. & Huang, P. *Biogeochemistry of Trace Elements in the Rhizosphere*. (Elsevier, 2011).
73. Magdziak, Z. et al. Influence of Ca/Mg ratio on phytoextraction properties of *Salix viminalis*. II. Secretion of low molecular weight organic acids to the rhizosphere. *Ecotoxicol. Environ. Saf.* **74**, 33–40 (2011).
74. Meier, S. et al. Influence of copper on root exudate patterns in some metallophytes and agricultural plants. *Ecotoxicol. Environ. Saf.* **75**, 8–15 (2012).
75. Chau, T. P. et al. Bioremediation efficiency of free and immobilized form of *Aspergillus niger* and *Aspergillus tubigenesis* biomass on tannery effluent. *Environ. Res.* **231**, 116275 (2023).
76. Pande, V., Pandey, S. C., Sati, D., Bhatt, P. & Samant, M. Microbial interventions in bioremediation of heavy metal contaminants in agroecosystem. *Front. Microbiol.* **13**, 824084 (2022).
77. Ouyang, P. et al. Integrating biochar and bacteria for sustainable remediation of metal-contaminated soils. *Biochar* **5**, 63 (2023).
78. Zhu, X. et al. The immobilization effects on Pb, Cd and Cu by the inoculation of organic phosphorus-degrading bacteria (OPDB) with rapeseed dregs in acidic soil. *Geoderma* **350**, 1–10 (2019).
79. Lai, W. et al. Combination of biochar and phosphorus solubilizing bacteria to improve the stable form of toxic metal minerals and microbial abundance in lead/cadmium-contaminated soil. *Agronomy* **12**, 1003 (2022).
80. Al-Hawash, A. B. et al. Principles of microbial degradation of petroleum hydrocarbons in the environment. *Egypt. J. Aquat. Res.* **44**, 71–76 (2018).
81. Das, N., Bhuyan, B. & Pandey, P. Correlation of soil microbiome with crude oil contamination drives detection of hydrocarbon degrading genes which are independent to quantity and type of contaminants. *Environ. Res.* **215**, 114185 (2022).
82. Devi, S. P., Jani, K., Sharma, A. & Jha, D. K. Bacterial communities and their bioremediation capabilities in oil-contaminated agricultural soils. *Environ. Monit. Assess.* **194**, 9 (2022).
83. Galitskaya, P., Biktasheva, L., Blagodatsky, S. & Selivanovskaya, S. Response of bacterial and fungal communities to high petroleum pollution in different soils. *Sci. Rep.* **11**, 164 (2021).
84. Tan, S. et al. A perspective on the interaction between biochar and soil microbes: A way to regain soil eminence. *Environ. Res.* **214**, 113832 (2022).
85. Lehmann, J. et al. Biochar effects on soil biota—A review. *Soil Biol. Biochem.* **43**, 1812–1836 (2011).
86. Oh, T.-K., Shinogi, Y., Chikushi, J., Lee, Y.-H. & Choi, B. Effect of aqueous extract of biochar on germination and seedling growth of lettuce (*Lactuca sativa* L.). (2012).
87. Amini, S., Ghadiri, H., Chen, C. & Marschner, P. Salt-affected soils, reclamation, carbon dynamics, and biochar: a review. *J. Soils Sediments* **16**, 939–953 (2016).
88. Qayyum, M. F., Steffens, D., Reisenauer, H. P. & Schubert, S. Kinetics of carbon mineralization of biochars compared with wheat straw in three soils. *J. Environ. Qual.* **41**, 1210–1220 (2012).
89. Prendergast-Miller, M. T., Duvall, M. & Sohi, S. P. Localisation of nitrate in the rhizosphere of biochar-amended soils. *Soil Biol. Biochem.* **43**, 2243–2246 (2011).
90. Egamberdieva, D. et al. The effect of biochars and endophytic bacteria on growth and root rot disease incidence of Fusarium infested narrow-leaved lupin (*Lupinus angustifolius* L.). *Microorganisms* **8**, 496 (2020).
91. Egamberdieva, D., Zoghi, Z., Nazarov, K., Wirth, S. & Bellingrath-Kimura, S. D. Plant growth response of broad bean (*Vicia faba* L.) to biochar amendment of loamy sand soil under irrigated and drought conditions. *Environ. Sustain.* **3**, 319–324 (2020).
92. Ma, H. et al. The integrated effect of microbial inoculants and biochar types on soil biological properties, and plant growth of lettuce (*Lactuca sativa* L.). *Plants* **11**, 423 (2022).
93. Ögüt, M., Er, F. & Neumann, G. Increased proton extrusion of wheat roots by inoculation with phosphorus solubilising microorganisms. *Plant Soil* **339**, 285–297 (2011).
94. Zou, Z. et al. Response of plant root growth to biochar amendment: a meta-analysis. *Agronomy* **11**, 2442 (2021).
95. Bidondo, L. F. et al. Differential interaction between two *Glomus intraradices* strains and a phosphate solubilizing bacterium in maize rhizosphere. *Pedobiologia* **55**, 227–232 (2012).
96. Nasslahsen, B., Prin, Y., Ferhout, H., Smouni, A. & Duponnois, R. Mycorrhizae helper bacteria for managing the mycorrhizal soil infectivity. *Front. Soil Sci.* **2**, 979246 (2022).
97. Cabello, M. N. Effectiveness of indigenous arbuscular mycorrhizal fungi (AMF) isolated from hydrocarbon polluted soils. *J. Basic Microbiol. Int. J. Biochem. Physiol. Genet. Morphol. Ecol. Microorg.* **39**, 89–95 (1999).
98. Swoczyna, T., Kalaji, H. M., Bussotti, F., Mojski, J. & Pollastrini, M. Environmental stress-what can we learn from chlorophyll fluorescence analysis in woody plants? A review. *Front. Plant Sci.* **13**, 1048582 (2022).
99. Aazami, M. A. et al. Low temperature stress mediates the antioxidants pool and chlorophyll fluorescence in *Vitis vinifera* L. cultivars. *Plants* **10**, 1877 (2021).
100. Ritchie, G. A. Chlorophyll fluorescence: What is it and what do the numbers mean. In *National Proceedings: Forest and Conservation Nursery Associations-2005*, 34–42 (2006).
101. Baker, N. R. & Rosenqvist, E. Applications of chlorophyll fluorescence can improve crop production strategies: an examination of future possibilities. *J. Exp. Bot.* **55**, 1607–1621 (2004).
102. Lichtenthaler, H., Buschmann, C. & Knapp, M. How to correctly determine the different chlorophyll fluorescence parameters and the chlorophyll fluorescence decrease ratio R_{Fd} of leaves with the PAM fluorometer. *Photosynthetica* **43**, 379–393 (2005).
103. Sperdoui, I. et al. Changes in light energy utilization in photosystem II and reactive oxygen species generation in potato leaves by the pinworm *Tuta absoluta*. *Molecules* **26**, 2984 (2021).
104. Moustakas, M., Bayçu, G., Sperdoui, I., Eroğlu, H. & Eleftheriou, E. P. Arbuscular mycorrhizal symbiosis enhances photosynthesis in the medicinal herb *Salvia fruticosa* by improving photosystem II photochemistry. *Plants* **9**, 962 (2020).

105. Sarvikas, P., Hakala, M., Pätsikkä, E., Tyystjärvi, T. & Tyystjärvi, E. Action spectrum of photoinhibition in leaves of wild type and npq1-2 and npq4-1 mutants of *Arabidopsis thaliana*. *Plant Cell Physiol.* **47**, 391–400 (2006).
106. Ripley, B. S., Redfern, S. P. & Dames, J. Quantification of the photosynthetic performance of phosphorus-deficient Sorghum by means of chlorophyll-a fluorescence kinetics. *S. Afr. J. Sci.* **100**, 615–618 (2004).
107. Van Heerden, P. D., Tsimilli-Michael, M., Krüger, G. H. & Strasser, R. J. Dark chilling effects on soybean genotypes during vegetative development: parallel studies of CO₂ assimilation, chlorophyll a fluorescence kinetics O-J-I-P and nitrogen fixation. *Physiol. Plant.* **117**, 476–491 (2003).
108. Fedeli, R., Alexandrov, D., Celletti, S., Nafikova, E. & Loppi, S. Biochar improves the performance of *Avena sativa* L. grown in gasoline-polluted soils. *Environ. Sci. Pollut. Res.* **30**, 28791–28802 (2023).
109. Rajput, V. D. et al. The influence of application of biochar and metal-tolerant bacteria in polluted soil on morpho-physiological and anatomical parameters of spring barley. *Environ. Geochem. Health* **43**, 1477–1489 (2021).
110. Achuba, F. & Iserhienrhien, L. Effects of soil treatment with abattoir effluent on morphological and biochemical profiles of cowpea seedlings (*V. unguiculata*) grown in gasoline polluted soil. *Ife J. Sci.* **20**, 51–59 (2018).
111. Njoku, K., Akinola, M. & Taiwo, B. Effect of gasoline diesel fuel mixture on the germination and the growth of *Vigna unguiculata* (Cowpea). *Afr. J. Environ. Sci. Technol.* **3** (2009).
112. Ezeonu, C. S. & Onwurah, I. Effect of crude oil contamination on Chlorophyll content in *Zea mays* L. *Int. J. Biol. Biotechnol.* **6**, 299–301 (2009).
113. Evans, J. R. Photosynthesis and nitrogen relationships in leaves of C3 plants. *Oecologia* **78**, 9–19 (1989).
114. Sage, R. F. & Percy, R. W. The nitrogen use efficiency of C3 and C4 plants: II. Leaf nitrogen effects on the gas exchange characteristics of *Chenopodium album* (L.) and *Amaranthus retroflexus* (L.). *Plant Physiol.* **84**, 959–963 (1987).
115. Dias, M. C., Pinto, D. C. & Silva, A. M. Plant flavonoids: Chemical characteristics and biological activity. *Molecules* **26**, 5377 (2021).
116. Li, Z. & Ahammed, G. J. Plant stress response and adaptation via anthocyanins: A review. *Plant Stress*. 100230 (2023).
117. Heidari, S., Fotouhi Ghazvini, R., Zavareh, M. & Kafi, M. Physiological responses and phytoremediation ability of Eastern Coneflower (*Echinacea purpurea*) for crude oil contaminated soil. *Caspian J. Environ. Sci.* **16**, 149–164 (2018).
118. Zhu, Y., Wang, H., Lv, X., Zhang, Y. & Wang, W. Effects of biochar and biofertilizer on cadmium-contaminated cotton growth and the antioxidative defense system. *Sci. Rep.* **10**, 20112 (2020).

Acknowledgements

Authors wish to thank Eurovix S.p.A. for providing bioactivators and Evergreen Resources S.r.l. for providing biochar. F. Pietrini and M. Zacchini wish to thank the National Recovery and Resilience Plan (NRRP), Mission 4 Component 2 Investment 1.4—Call for tender No. 3138 of December 16, 2021, rectified by Decree n.3175 of December 18, 2021 of Italian Ministry of University and Research funded by the European Union—NextGenerationEU; Award Number: Project code CN_00000033, Concession Decree No. 1034 of June 17, 2022 adopted by the Italian Ministry of University and Research, CUPB83C22002930006, Project title “National Biodiversity Future Center—NBFC”.

Author contributions

V.M.-M.: Resources, investigation, data curation, visualization, writing—original draft, writing—review and editing. L.P.: Conceptualization, resources, methodology, investigation, data curation, writing—original draft, writing—review and editing. M.Z.: Resources, methodology, writing review and editing. F.P.: Investigation, formal analysis, visualization, writing—original draft, writing review and editing. E.P.: Methodology, investigation, writing—original draft. S.C.: Resources, investigation. L.R.: Investigation, data curation. G.G.: Investigation, data curation. A.B.C.: Resources, writing—review and editing, validation. V.S.: Investigation, data curation, visualization, writing—original draft. M.C.M.: Investigation. R.M.: Investigation, data curation L.M.: Investigation, data curation, writing—original draft. S.M.: Resources, writing—review and editing, funding acquisition. I.N.: Conceptualization, resources, methodology, formal analysis, writing—original draft, writing—review and editing, supervision.

Declarations

Competing interests

The authors declare no competing interests.

Consent to publish

All authors agreed with the content, all gave explicit consent for submission, and all obtained approval from the relevant authorities at the institution where the work was carried out before submission.

Additional information

Supplementary Information The online version contains supplementary material available at <https://doi.org/10.1038/s41598-025-93879-5>.

Correspondence and requests for materials should be addressed to L.P.

Reprints and permissions information is available at www.nature.com/reprints.

Publisher's note Springer Nature remains neutral with regard to jurisdictional claims in published maps and institutional affiliations.

Open Access This article is licensed under a Creative Commons Attribution-NonCommercial-NoDerivatives 4.0 International License, which permits any non-commercial use, sharing, distribution and reproduction in any medium or format, as long as you give appropriate credit to the original author(s) and the source, provide a link to the Creative Commons licence, and indicate if you modified the licensed material. You do not have permission under this licence to share adapted material derived from this article or parts of it. The images or other third party material in this article are included in the article's Creative Commons licence, unless indicated otherwise in a credit line to the material. If material is not included in the article's Creative Commons licence and your intended use is not permitted by statutory regulation or exceeds the permitted use, you will need to obtain permission directly from the copyright holder. To view a copy of this licence, visit <http://creativecommons.org/licenses/by-nc-nd/4.0/>.

© The Author(s) 2025